12/15-Lipoxygenase metabolites of arachidonic acid activate PPARγ: a possible neuroprotective effect in ischemic brain

Li Sun,[1] Yan-Wei Xu, Jing Han, Hao Liang, Ning Wang, and Yan Cheng

Tianjin Medical University General Hospital, Tianjin Neurological Institute, Key Laboratory of Post-trauma Neuro-repair and Regeneration in Central Nervous System, Ministry of Education, Tianjin Key Laboratory of Injuries, Variations and Regeneration of Nervous System, Tianjin, 300052, People's Republic of China

Abstract The enzyme 12/15-lipoxygenase (LOX) oxidizes various free fatty acids, including arachidonic acid (AA). In the brain, the principal 12/15-LOX metabolites of AA are 12(S)-HETE and 15(S)-HETE. PPARγ is a nuclear receptor whose activation is neuroprotective through its anti-inflammatory properties. In this study, we investigate the involvement of 12(S)- and 15(S)-HETE in the regulation of PPARγ following cerebral ischemia and their effects on ischemia-induced inflammatory response. We show here the increased expression of 12/15-LOX, predominantly in neurons, and elevated production of 12(S)-HETE and 15(S)-HETE in ischemic brain. The exogenous 12(S)- and 15(S)-HETE increase PPARγ protein level, nuclear translocation, and DNA-binding activity in ischemic rats, suggesting the activation of PPARγ. This effect was further confirmed by showing the increased PPARγ transcriptional activity in primary cortical neurons when incubated with 12(S)- or 15(S)-HETE. Moreover, both 12(S)- and 15(S)-HETE potently inhibited the induction of nuclear factor-κB, inducible NO synthase, and cyclooxygenase-2 in ischemic rats, and elicited neuroprotection. The reversal of the effects of 12(S)- and 15(S)-HETE on pro-inflammatory factors by PPARγ antagonist GW9662 indicated their actions were mediated via PPARγ. Thus, the induction of 12(S)- and 15(S)-HETE during brain ischemia suggests that endogenous signals of neuroprotection may be generated.—Sun, L., Y-W. Xu, J. Han, H. Liang, N. Wang, and Y. Cheng. **12/15-Lipoxygenase metabolites of arachidonic acid activate PPARγ: a possible neuroprotective effect in ischemic brain.** ***J. Lipid Res.*** **2015.** 56: **502–514.**

Supplementary key words peroxisome proliferator-activated receptor γ • hydroxyeicosatetraenoic acid • brain ischemia

12/15-Lipoxygenase (LOX) is a lipid-peroxidating enzyme that promotes a variety of polyunsaturated fatty acids to form a series of biologically active lipid mediators (1, 2). In the CNS, 12/15-LOX expression has been described throughout the cerebrum, basal ganglia, and hippocampus (3, 4). Arachidonic acid (AA) is an important component of membrane lipids that can activate several signaling pathways directly by itself or by its metabolites (5). In nervous tissue, the major enzymatic route for AA metabolism is the 12/15-LOX pathway, and the principal metabolites are 12(S)-HETE and 15(S)-HETE (3, 4, 6, 7). The biological significance of these metabolites of AA is that they have been proposed to play roles as second messengers in synaptic transmission and they are thought to be involved in learning and memory processes (8). In addition, 12(S)-HETE is known to act as an inhibitory neuromodulator by reducing voltage-sensitive calcium channel activity (9) and attenuating glutamate release and affinity to its receptors (10–12).

Brain ischemia triggers the massive release of free fatty acids from membrane stores, such as AA and DHA, and then the accumulation of lipid peroxides. 12/15-LOX is thought to be damaging because of its lipid-oxidizing properties, and the detrimental effects of 12/15-LOX have been documented by demonstrating the protection in the ischemic brain through 12/15-LOX inhibition or gene deletion (13–15). Several metabolites of 12/15-LOX, however, have neuroprotective and anti-inflammatory qualities during brain ischemia. For example, 12/15-LOX metabolites derived from DHA and other ω-3 fatty acids inhibit cerebral ischemia-induced injury (16–18). This suggests 12/15-LOX and its metabolites may differ in their effects following cerebral ischemia.

PPARγ is a member of the nuclear hormone receptor family of ligand-dependent transcription factors. PPARγ

This work was supported by grants from the National Natural Science Foundation of China (number 81070968 to L.S. and number 81401023 to Y-W.X.) and from the Tianjin Municipal Science and Technology Commission (number 13ZCZDSY01900 to Y.C.). The authors declare no conflicts of interest.

Manuscript received 15 July 2014 and in revised form 7 January 2015.

Published, JLR Papers in Press, January 20, 2015
DOI 10.1194/jlr.M053058

Abbreviations: AA, arachidonic acid; COX-2, cyclooxygenase-2; HPETE, hydroperoxyeicosatetraenoic acid; iNOS, inducible NO synthase; LOX, lipoxygenase; MCAO, middle cerebral artery occlusion; NeuN, neuronal nuclei; NF-κB, nuclear factor-κB; nitrate/nitrite, nitrate plus nitrite; PPRE, peroxisome proliferator response element; TTC, 2,3,5-triphenyltetrazolium chloride.

[1]To whom correspondence should be addressed.
e-mail: sunli_2000@hotmail.com

regulates genes that are implicated in adipocyte differentiation, lipid and glucose metabolism, and insulin sensitivity. PPARγ also plays a central role in dampening inflammation via its inhibitory activity on expression of the pro-inflammatory mediators (19–21). Notably, treatment of rats with the ligands of PPARγ can significantly protect the brain from ischemic insult by acting against inflammatory responses (22–27). For example, in the transient middle cerebral artery occlusion (MCAO) model of the rat, administration of PPARγ ligands troglitazone or pioglitazone dramatically decreased infarction volume, attenuated microglia activation, and reduced the expression of interleukin-1β (IL-1β), cyclooxygenase-2 (COX-2), and inducible NO synthase (iNOS) (22). Another PPARγ agonist, rosiglitazone, also shows potent anti-inflammatory actions following transient focal ischemia by inhibiting the expression of pro-inflammatory proteins, myeloperoxidase and intercellular adhesion molecule-1 (ICAM-1), and reduced neutrophil accumulation (25). Recently, it has been found that 12(S)- and 15-(S)-HETE can function as ligands of PPARγ in the cells derived from outside the CNS (28–32). However, whether they can regulate PPARγ following brain ischemia is still unknown. Moreover, AA itself has been shown to be neuroprotective against oxidative stress on hippocampal slices and furthermore, its neuroprotective effect was completely abolished by PPARγ antagonist, suggesting the involvement of activation of PPARγ (33). Accordingly, we hypothesize that 12(S)- and 15-(S)-HETE production following cerebral ischemia may be of beneficial effect by regulating PPARγ. Using a rat model of focal cerebral ischemia, we explored whether exogenous administration of 12(S)- and 15(S)-HETE could activate PPARγ and thus demonstrate the anti-inflammatory properties in ischemic brain.

EXPERIMENTAL PROCEDURES

Rat model of transient focal ischemia

All studies were conducted after gaining the approval of the Animal Care and Use Committee of Tianjin Medical University. Male Sprague-Dawley rats (Academy of Military Medical Sciences, Beijing, China) weighing from 280 to 330 g were fasted overnight, but were allowed free access to water. Animals were anesthetized with 3% halothane and anesthesia was maintained with 1.5% halothane in 30% oxygen and 68.5% nitrous oxide delivered by facemask. Cerebral ischemic injury was induced by the intraluminal MCAO method as described previously (34). Briefly, the left MCAO was induced by intraluminally advancing a suture with silicone-coated tip to block the origin of the middle cerebral artery. After 90 min occlusion, the animals were again anesthetized with 3% halothane and anesthesia was maintained with 1.5% halothane in 30% oxygen and 68.5% nitrous oxide delivered by facemask. The neck incision was reopened and the suture was removed to allow reperfusion for an indicated duration. Regional cerebral blood flow was measured by laser Doppler flowmetry before and during MCAO, as well as after reperfusion. Systolic arterial blood pressure was monitored through tail-cuff plethysmography. Rectal temperature was continuously maintained (37.5 ± 0.5°C) using a temperature-regulated heating pad and a heating lamp on the surgery table. The femoral artery was catheterized for analysis of blood gases. All animals survived the MCAO surgical procedure. Rats that did not demonstrate neurological deficits during 90 min MCAO were excluded from further study. Animals dying prematurely during the reperfusion period or having subarachnoid hemorrhage at postmortem examination were also excluded. Measurements derived from these animals were not included in the present study.

Drug treatment

Eicosanoids, 12(S)-HETE and 15(S)-HETE, were products of Cayman Chemical (Ann Arbor, MI) and given 30 min before the onset of MCAO by icv injection. 12(S)- and 15(S)-HETE, supplied in ethanol at 1 mg/ml, were air-dried under a stream of nitrogen and dissolved in a 30% DMSO and 70% isotonic saline solution (35). Animals received either vehicle (30% DMSO-0.9% saline) or a single dose of 12(S)- or 15(S)-HETE at 10, 15, or 20 μg (~31–62 nmol) per injection. This dosing regimen was chosen to resemble that previously shown to confer neuroprotection and activation of PPARγ by a natural PPARγ ligand, 15d-PGJ2 (35, 36). Briefly, anesthetized rats were placed in a stereotaxic apparatus; 12(S)- or 15(S)-HETE in 10 μl of vehicle per injection was infused into the left lateral brain ventricle using the following coordinates: 0.8 mm posterior to bregma, 1.3 mm lateral from midline, and 3.5 mm below the dural surface. All the substances were injected at a rate of 1 μl/min using a syringe pump. In some experiments, the rats were pretreated with the PPARγ antagonist, GW9662 (Cayman Chemical). GW9662 was dissolved in 3% DMSO and administered ip at a dose of 1, 2, or 4 mg/kg 30 min before 12(S)- or 15(S)-HETE treatment and the subsequent MCAO. Control groups were injected with either 30% DMSO-0.9% saline (icv), 3% DMSO (ip), or both, based on the experiment. The effect of vehicle without any drug was tested in pilot experiments; no effects were observed. Eight animals were observed in each treatment.

Tissue preparation and nuclear extract isolation

Tissues representing the ipsilateral cortices were harvested at the indicated time after the 90 min ischemia. The tissues were homogenized at 4°C in PBS containing protease inhibitors (10 μg/ml soybean trypsin inhibitor, 10 μg/ml benzamidine, 10 μg/ml aprotinin, 10 μg/ml leupeptin, 10 μg/ml pepstatin A, 5 μg/ml antipain, 0.2 mM PMSF, 0.1 mM ethylene diamine tetra-acetic acid). Each sample was homogenized and sonicated on ice. The homogenates were centrifuged at 3,000 *g* for 15 min at 4°C, and supernatant was obtained and used for total protein analysis.

Nuclear and cytoplasmic fractions were separated with the Active Motif nuclear extract kit (Carlsbad, CA). Isolated brain tissue was finely diced and homogenized in ice-cold buffer, and the manufacturer's instructions were followed. Both fractions were applied for Western blot analysis of PPARγ subcellular fractions, and the nuclear extract protein was also used for the assay of DNA binding activity of transcription factors.

Western blot analysis

Proteins were separated on 8% SDS-PAGE, and then transferred onto nitrocellulose membrane. After blocking for 1 h in 0.1% Tween 20/PBS (PBS-T) containing 5% fat-free milk, the blot was incubated with the primary antibody at 4°C overnight. The antibodies were anti-PPARγ (1:200 dilution; Santa Cruz Biotechnology, Santa Cruz, CA), anti-12/15-LOX (1:1,000 dilution; Cayman Chemical), anti-COX-2 (1:1,000 dilution; Santa Cruz Biotechnology), or anti-iNOS (1:200 dilution; Santa Cruz Biotechnology). After three washings with PBS-T, the membranes were incubated for 1 h at room temperature with appropriate HRP-conjugated secondary antibodies. The blot was visualized by chemiluminescence. The density of the bands was evaluated

densitometrically using the program Quantity One 4.6.2 (Bio-Rad Laboratories, Hercules, CA).

Immunohistochemistry

For single-label immunohistochemistry, frozen sections were permeabilized with 0.3% (v/v) Triton X-100 in PBS for 30 min and blocked with 1% (w/v) BSA in PBS for 1 h, then incubated with primary antibody for 12/15-LOX (1:100, Cayman Chemical) at 4°C overnight. After washing six times in PBS, sections were incubated with FITC-labeled secondary antibody for 1 h at 37°C in the dark. Washing again for six times in PBS, sections were exposed to 4',6-diamidino-2-phenylindole (Beyotime Institute of Biotechnology, China) in the dark at room temperature for 10 min. The fluorescent images were observed under a fluorescent microscope. For double fluorescent staining, fresh-frozen sections were used and incubated with antibodies for 12/15-LOX and marker protein for neurons (neuronal nuclei, NeuN) separately. The first primary antibody was sheep anti-12/15-LOX antibody (1:100 dilution, Cayman Chemical) and the first secondary antibody was FITC-conjugated rabbit anti-sheep IgG (1:200 dilution, Invitrogen, Carlsbad, CA). The second primary antibody was mouse anti-NeuN antibody (1:100 dilution, Chemicon International) and the second secondary antibody was Texas Red-conjugated horse anti-mouse IgG (1:200 dilution, Vector Laboratories).The immunoreactivity of 12/15-LOX and NeuN was demonstrated as red and green fluorescence, respectively. The specificity of staining was confirmed using nonimmune control IgG (data not shown).

Measurement of 12(S)-HETE and 15(S)-HETE

For assessment of 12(S)-HETE and 15(S)-HETE, brain samples were homogenized on ice in 50 mM phosphate buffer (pH 7.4). The homogenates were centrifuged at 10,000 *g* for 20 min at 4°C. Measurements were performed with the 12(S)-HETE and 15(S)-HETE enzyme immunoassay kits (Assay Designs, Ann Arbor, MI), respectively, in accordance with the manufacturer's instructions. The kits use a polyclonal antibody against 12(S)-HETE or 15(S)-HETE in both free and esterified forms in the samples. Results are expressed in nanograms per milligram of protein.

DNA binding activity assay

To assess the level of PPARγ DNA binding induced by 12(S)-HETE or 15(S)-HETE, the TransAM PPARγ transcription factor assay kit (Active Motif) was performed following the manufacturer's instructions. The kit consists of a double-stranded DNA sequence containing the peroxisome proliferator response element (PPRE) immobilized to the wells of a 96-well plate. Nuclear extracts from the ischemic cortex were prepared with the Active Motif nuclear extract kit. Immunoblotting of GAPDH was used to detect cytoplasmic contamination in nuclear extracts. After that, 10 μg of nuclear extract protein was applied to the wells and allowed to bind to the PPRE. Then, PPARγ primary antibody and HRP-conjugated secondary antibody were sequentially added. A colorimetric readout was obtained at 450 nm using a Bio-Rad plate reader. The specificity of the assay was confirmed by the addition of wild-type and mutated consensus oligonucleotides. The wild-type consensus oligonucleotide can prevent PPARγ binding to the probe immobilized on the 96-well plate and eliminated the signals, whereas the mutated consensus oligonucleotide has little effect on PPARγ binding. Similarly, the DNA binding activity of nuclear factor-κB (NF-κB) was determined using the TransAM NF-κB (p65) transcription factor assay kit (Active Motif) to detect the activation of this transcription factor.

Primary culture of cortical neurons

Primary cortical neurons were prepared from embryonic day 17 Sprague-Dawley rats as described (34). Briefly, cells were dissociated from the cortex, digested with trypsin (Invitrogen), followed by gentle trituration to release cells. After washing, cells were maintained in serum-free B27 neurobasal media (Invitrogen) in a humidified atmosphere of 5% CO_2/95% air at 37°C. All experiments were performed with neurons that had been in culture for 7–9 days in vitro. Neuron purity was determined using MAP2 labeling, a cell marker for neurons (37), which showed >95% purity in cultures.

Plasmids and transient transfection

PPARγ transcriptional activity was evaluated by transient transfection of an expression vector containing the PPRE, the oligonucleotide which PPARγ specifically binds to. The oligonucleotide corresponding to PPRE of rat acyl CoA oxidase (38) was used: 5′-TGACCTTTGTCCT-3′. The 3×PPRE-Luc plasmid was constructed by inserting three copies of the PPRE into the luciferase reporter vector, pGL3-Basic (Promega, Madison, WI) using the enzymes KpnI-*Hin*dIII. The construct was then confirmed by DNA sequencing. Transient transfection of neurons was performed as described (39) using Lipofectamine 2000 (Invitrogen). Briefly, neurons were seeded in 24-well plates at a density of ∼4–5 × 10^5 cells/well and transiently transfected with 1 μg of plasmid DNA in each well. At 24 h after transfection, neuronal cells were then treated with increasing concentrations of 12(S)-HETE or 15(S)-HETE for an additional 24 h. Luciferase activity was measured using the Luciferase Assay system (Promega). Transfection efficiency was evaluated by the basis of β-galactosidase activity levels. All reporter assays were performed in three replicates in eight independent experiments.

Nitrate plus nitrite measurement

The total amount of NO end production, nitrate plus nitrite (nitrate/nitrite), was measured using a commercially available kit from Cayman Chemical, as described previously (34). Briefly, samples of brain cortical tissue were sonicated in ice-cold PBS (pH 7.4) for 15 s and then centrifuged at 10,000 *g* for 20 min. The supernatant solution was then ultracentrifuged at 100,000 *g* for 30 min, followed by filtering through a 30 kDa molecular mass cut-off filter. Absorbance was measured at 540 nm and converted to nitrate/nitrite content by using a nitrate standard curve. Data are expressed as nanomoles of nitrate/nitrite per milligram of protein.

Measurement of infarct volume

Infarct volumes were measured using 2,3,5-triphenyltetrazolium chloride (TTC) (Sigma Chemical) staining. Brains were quickly removed and cut into 2 mm-thick coronal sections. The slices were incubated in 2% TTC at 37°C for 20 min to visualize the infarctions. An image of each slice was analyzed with the Image Pro Plus 6.0 software. To correct for brain swelling in infarction size calculations, the area of uninfarcted tissue in the ischemic hemisphere was measured and subtracted from the area of the intact contralateral hemisphere. The area of infarction from each slice was summed and presented as a percentage of the volume of the uninfarcted hemisphere.

Assessment of neurological deficits

Assessment of neurological deficits was performed in animals using a standard scoring system: 0, no defect; 1, failure to extend right forepaw; 2, circling to right; 3, falling to right; and 4, inability to walk spontaneously.

Statistical analysis

The experimental data are expressed as mean ± SEM and SPSS 11.0 software package was used for data processing. One-way ANOVA was used to compare the means of different groups. Comparisons between two groups were conducted by *t*-test. A P value <0.05 was considered as statistically significant.

RESULTS

Cerebral ischemia induces elevation of 12/15-LOX expression and metabolites 12(S)- and 15(S)-HETE levels

We first investigated 12/15-LOX, the 12(S)- and 15(S)-HETE-producing enzyme, expression in a rat model of transient focal ischemia induced by MCAO. Following 90 min of ischemia, there was a progressive increase in 12/15-LOX protein level in the ischemic brain (ipsilateral cortex) detected by Western blot analysis (**Fig. 1A**). This increase occurred as early as 4 h after MCAO and became dramatic from 24 h. To examine the spatial localization of the increase in 12/15-LOX, the immunoreactivity of 12/15-LOX was visualized by immunohistochemical analysis. As illustrated in Fig. 1B, the immunoreactivity of 12/15-LOX was localized primarily to the ischemic border zone at 24 h after MCAO. There was only a little 12/15-LOX expression on the contralateral side. Incubation without the primary antibody resulted in the complete lack of staining (data not shown). To determine whether neurons give rise to the 12/15-LOX signal, we carried out double-labeling experiments with a NeuN. The 12/15-LOX signal was clearly overlaid with strong NeuN immunoreactivity (Fig. 1C), suggesting that the increased 12/15-LOX is likely a result of the neuronal response to ischemic injury.

The 12(S)- and 15(S)-HETE synthesis was also evaluated in the ischemic brain. Consistent with the changes in 12/15-LOX expression, the content of total 12(S)- or 15(S)-HETE in the ipsilateral cortex was time-dependently increased following 90 min ischemia (Fig. 1D).

12(S)-HETE and 15(S)-HETE enhance ischemia-induced PPARγ expression and activity

To ascertain whether PPARγ was regulated by the 12/15-LOX metabolites of AA, exogenous 12(S)- or 15(S)-HETE (10, 15, and 20 μg) was given 30 min before the

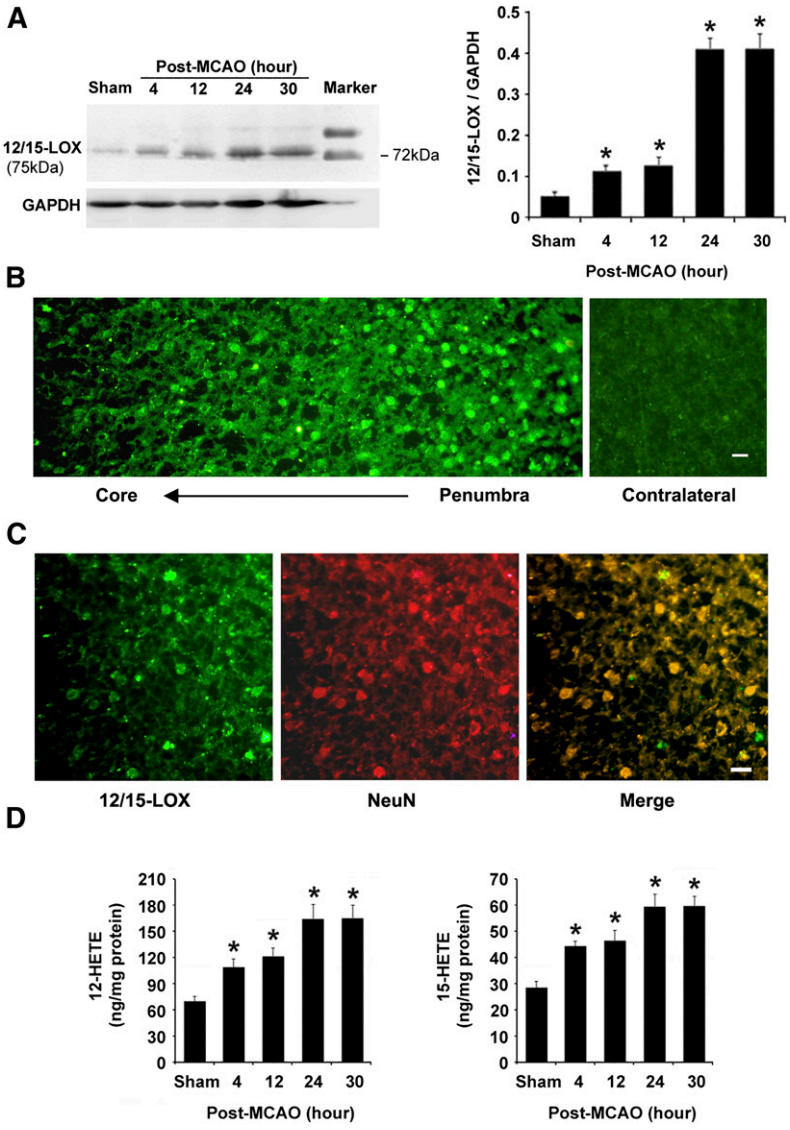

Fig. 1. 12/15-LOX expression and metabolites 12(S)- and 15(S)-HETE were upregulated in ischemic brain. Focal ischemia was induced by transient MCAO. A: Western blot analysis of 12/15-LOX expression (75 kDa) in ipsilateral (ischemic) cortex at indicated time points after 90 min MCAO. The bar graph indicates the densitometric values of 12/15-LOX protein (normalized to GAPDH levels). Data are expressed as mean ± SEM; n = 8/group; *P < 0.05 versus sham-operated rats (Sham). B: Fluorescent immunohistochemical staining of 12/15-LOX in the frontoparietal cortex of rats at 24 h post-MCAO. Representative images show cerebral cortex representing ischemic core, ischemic penumbra, and contralateral homotopic cortex. Scale bar, 20 μM. C: Double fluorescent labeling of 12/15-LOX (green fluorescence) and NeuN (red fluorescence) in frontoparietal cortex at 24 h after MCAO. Representative images show the 12/15-LOX- and NeuN-positive cells. Scale bar, 20 μM. D: The content of 12/15-LOX metabolites 12(S)- and 15(S)-HETE in ipsilateral (ischemic) cortex. Values are expressed as nanograms per milligram protein. n = 8/group; *P < 0.05 versus Sham.

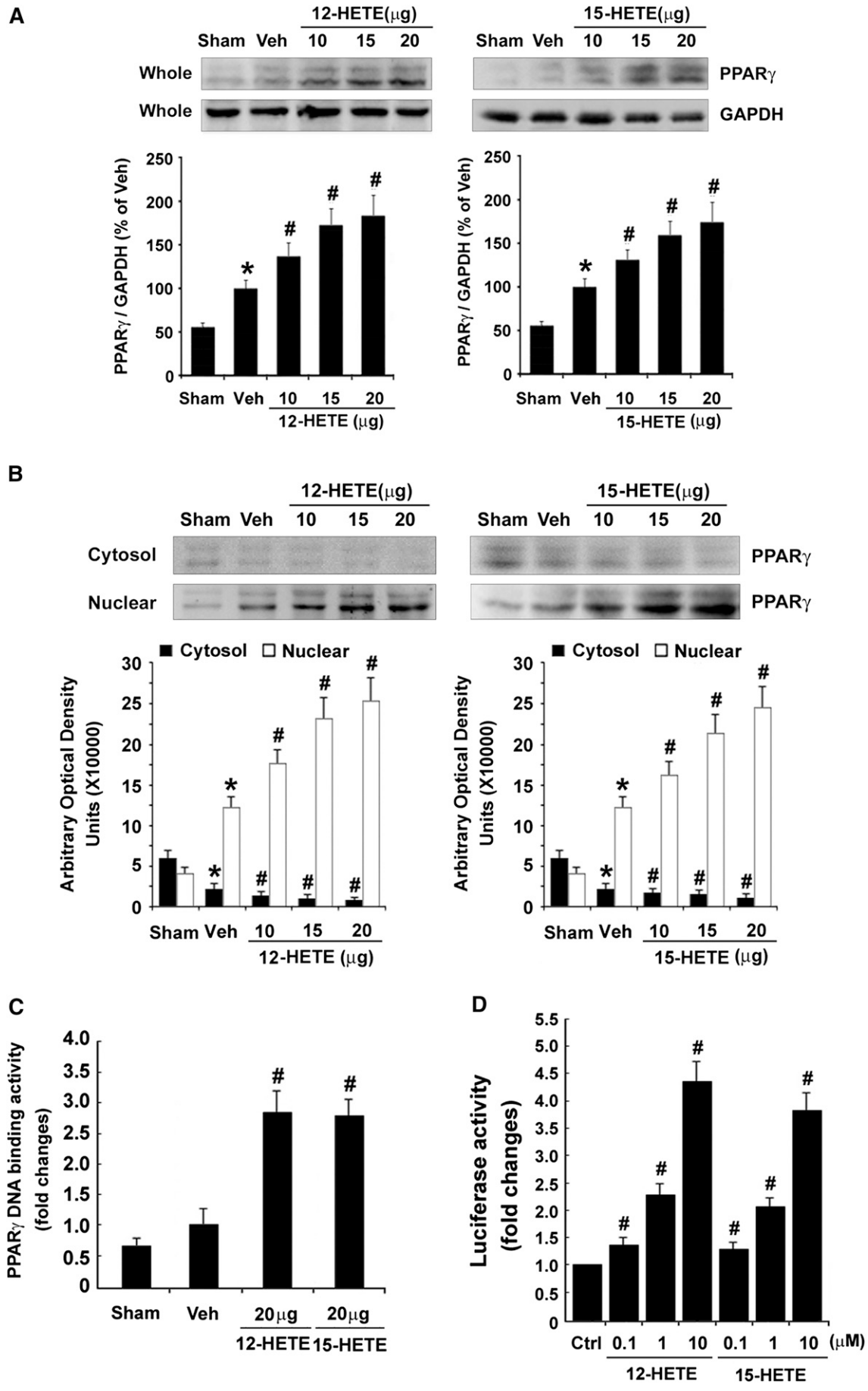
A
12-HETE(μg)
Sham Veh 10 15 20
Whole
Whole
15-HETE(μg)
Sham Veh 10 15 20
PPARγ
GAPDH
PPARγ / GAPDH (% of Veh)
Sham Veh 10 15 20
12-HETE (μg)
15-HETE (μg)
B
Cytosol
Nuclear
Arbitrary Optical Density Units (X10000)
C
PPARγ DNA binding activity (fold changes)
Sham Veh 20μg 20μg
12-HETE 15-HETE
D
Luciferase activity (fold changes)
Ctrl 0.1 1 10 0.1 1 10 (μM)
12-HETE 15-HETE

onset of MCAO by icv injection. At 24 h after ischemia, the whole protein lysate and cytosol and nuclear protein fractions were isolated from the ipsilateral cortex. Western blot analysis revealed that ischemic injury induced PPARγ whole protein upregulation (**Fig. 2A**) and cytoplasm-to-nuclear translocation (Fig. 2B) when compared with the sham-operated control. The exposure to either 12(S)- or 15(S)-HETE could further increase PPARγ total protein level (Fig. 2A) and nuclear translocation (Fig. 2B), indicating the activation of PPARγ.

To confirm this issue, we next performed an ELISA-based assay to examine the specific DNA binding activity of PPARγ. For this purpose, the nuclear extract proteins from the rats treated with 12(S)-HETE, 15(S)-HETE, or vehicle were incubated in a 96-well plate immobilized with an oligonucleotide containing the PPRE. As demonstrated in Fig. 2C, both 12(S)- and 15(S)-HETE treatment (20 μg) significantly increased the DNA binding activity of PPARγ compared to treatment with vehicle. Administration of 12(S)- or 15(S)-HETE to sham-operated rats only slightly increased PPARγ whole protein expression and DNA binding activity compared with nonpretreated sham-operated rats (data not shown).

Finally, we assessed PPARγ transcriptional activity in neuronal cells, the cell type in which both 12/15-LOX and PPARγ are predominantly expressed (14, 15, 36, 40) and PPARγ deficiency increases susceptibility to brain ischemic damage (26). Primary cultured cortical neurons were transiently transfected with a luciferase reporter construct containing three copies of a consensus PPRE and treated with increasing concentrations of 12(S)- or 15(S)-HETE. The luciferase activity was assayed and the results were presented in Fig. 2D. Upon exposure to 12(S)- or 15(S)-HETE (0.1, 1, and 10 μM) (41, 42), the expression of the reporter gene luciferase was increased in a dose-dependent manner. This observation thus confirmed that 12(S)- and 15(S)-HETE increase the transcriptional activity of endogenous PPARγ.

The effects of 12(R)- or 15(R)-HETE, the isomers of 12(S)- or 15(S)-HETE with opposing chirality, on PPARγ activation were also examined. The (R) isomers of HETEs failed to show any significant effects on either PPARγ DNA binding activity or PPARγ transcriptional activity (data not shown).

12(S)-HETE and 15(S)-HETE inhibit ischemia-induced upregulation of COX-2 and iNOS, as well as NF-κB activation

During brain ischemia, overexpression of COX-2 and iNOS have recently emerged as important determinants of postischemic inflammation, which contributes to the progression of brain damage (43, 44), whereas PPARγ activation is able to inhibit ischemia-induced inflammatory response (22–27). We therefore evaluated whether exogenous 12(S)- and 15(S)-HETE could suppress the induction of COX-2 and iNOS by ischemic injury. The levels of COX-2 and iNOS proteins were determined by Western blotting and NO release from iNOS was detected by Griess reaction at 24 h after ischemia. As shown in **Fig. 3A**, the levels of both COX-2 and iNOS increased several-fold in vehicle-treated brains (ipsilateral/ischemic cortex) as compared with sham-operated nonischemic brains. 12(S)- or 15(S)-HETE treatment (10, 15, and 20 μg) significantly attenuated COX-2 and iNOS expression in a dose-dependent manner. The effects of 12(S)- and 15(S)-HETE on iNOS protein levels were also paralleled by a significant reduction in NO levels in the ischemic cortex, as evaluated by the content of NO end product nitrate/nitrite (Fig. 3B). Twenty-four hours after MCAO, we also measured DNA binding activity of NF-κB as a marker for NF-κB activation. NF-κB was increased over 2-fold in the ipsilateral cortex, and the infusion of 12(S)- or 15(S)-HETE (20 μg) significantly inhibited ischemia-induced NF-κB activation, respectively (Fig. 3C). Administration of 12(S)- or 15(S)-HETE to sham-operated rats had no significant effect on any of the measured markers compared with rats that underwent only sham operation (data not shown).

PPARγ antagonist, GW9662, dose-dependently reverses the suppressive effects of 12(S)-HETE and 15(S)-HETE on COX-2, iNOS, and NF-κB

We next investigated whether the anti-inflammatory effects of 12(S)- and 15(S)-HETE could be reversed by the selective PPARγ antagonist, GW9662. Rats were injected with GW9662 (1, 2, and 4 mg/kg) 30 min before the 12(S)- or 15(S)-HETE treatment (20 μg) and the subsequent MCAO exposure. As illustrated in **Fig. 4A**, GW9662 dose-dependently abrogated the suppressive effects of 12(S)- and 15(S)-HETE on COX-2 and iNOS expression. A similar reversal of the inhibition in NO production was also observed by the treatment of increasing concentrations of GW9662 (Fig. 4B). In addition, GW9662 dose-dependently reversed the effect of 12(S)- or 15(S)-HETE-elicited decrease of NF-κB activation in ischemic brain (Fig. 4C). These data indicate that the inhibitory effects of 12(S)- and 15(S)-HETE on these pro-inflammatory mediators are PPARγ dependent. Administration of GW9662 to sham-operated animals had no effect on any of the measured markers (data not shown).

Fig. 2. 12(S)-HETE and 15(S)-HETE increased PPARγ expression and activity in ischemic brain. Focal ischemia was induced by transient MCAO. A–C: 12(S)-HETE or 15(S)-HETE (10, 15, and 20 μg) or vehicle was injected icv 30 min before the onset of MCAO. The whole protein lysate of ischemic cortex was extracted at 24 h after MCAO. The cytosol and nuclear fractions were isolated as described in the Experimental Procedures. PPARγ protein level (A) was measured by Western blot analysis with the whole protein lysate. PPARγ nuclear translocation (B) was evaluated with cytosol and nuclear protein fractions. The bar graph illustrates the densitometric analysis of the related bands. PPARγ DNA binding activity (C) was detected utilizing the PPARγ transcription factor assay kit. Data are expressed as mean ± SEM; n = 8/group; $*P < 0.05$ versus sham-operated rats (Sham), $\#P < 0.05$ versus vehicle-treated ischemic rats (Veh). D: PPARγ transcriptional activity was observed by luciferase activity assay in cultured cortical neurons transfected with a 3×PPRE-Luc construct. Increasing concentrations of 12(S)-HETE or 15(S)-HETE (0.1, 1, and 10 μM) were exogenously added to the cells, and 24 h later the luciferase activity was measured in control (Ctrl) and HETE-treated cells, respectively. n = 8; $\#P < 0.05$ versus control.

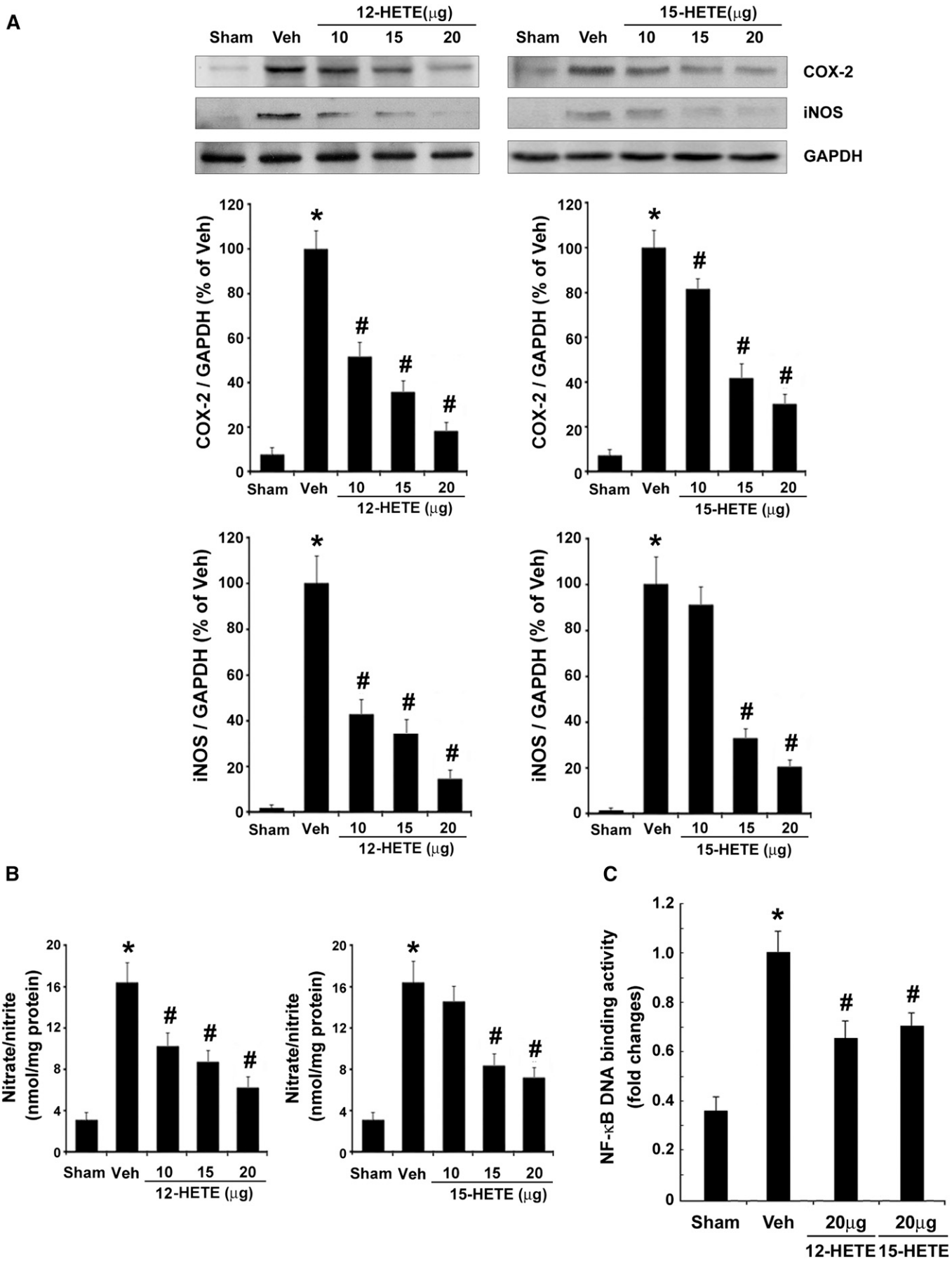
A
12-HETE(μg)
15-HETE(μg)
Sham
Veh
10
15
20
COX-2
iNOS
GAPDH
COX-2 / GAPDH (% of Veh)
iNOS / GAPDH (% of Veh)
12-HETE (μg)
15-HETE (μg)
B
Nitrate/nitrite (nmol/mg protein)
C
NF-κB DNA binding activity (fold changes)
20μg
12-HETE
15-HETE

12(S)-HETE and 15(S)-HETE elicit neuroprotection in rats exposed to focal ischemia

As the anti-inflammatory effect of PPARγ activation contributes to its protection from cerebral ischemic injury (22–27), we next investigated whether the two metabolites could afford neuroprotection in rats exposed to MCAO. Infarct volume was measured at 24 h after 90 min MCAO by TTC staining. TTC is actively taken up by cells into mitochondria resulting in a reddish color in normal tissue, whereas the infracted area is colorless. The focal infarcted volume in rats infused with vehicle was about 30% of the hemisphere. The infusion of 12(S)-HETE or 15(S)-HETE (20 μg) significantly reduced infarct volume to 18.23% and 20.07%, respectively (**Fig. 5A**). Neurological deficits were examined and scored on a grading scale of zero to four. Before MCAO, the neurologic score was normal (score = 0) in all animals. At 24 h after ischemia, vehicle-treated rats exhibited significant neurological impairments. 12(S)-HETE or 15(S)-HETE treatment significantly reduced ischemia-induced neurological deficits (scores: 2.75 ± 0.25 vs. 1.13 ± 0.22 in vehicle and 12-HETE, respectively; 2.75 ± 0.25 vs. 1.38 ± 0.18 in vehicle and 15-HETE, respectively, n = 8, $P < 0.05$) (Fig. 5B). Blood pressure, arterial blood gases, and rectal temperature were equivalent among groups of animals (data not shown).

DISCUSSION

Our findings reported here suggest a possible effect of 12/15-LOX metabolites of AA in ischemic brain: activation of PPARγ and thereby inhibition of inflammatory response. In the present study, we showed the increments in both 12/15-LOX expression and its metabolites 12(S)- and 15(S)-HETE levels in ischemic brain, which is consistent with the reports of others (13–15). Treatment with exogenous 12(S)- and 15(S)-HETE can activate PPARγ, respectively, and potently inhibit the induction of pro-inflammatory factors in a PPARγ-dependent manner. Moreover, the infusion of these metabolites elicits neuroprotection by reducing infarct size and improving neurological deficits. These findings indicate that the production of 12(S)- and 15(S)-HETE by 12/15-LOX is associated with activation of PPARγ and this event may be protective against cerebral ischemic injury.

There is a considerable literature describing the activation of PPARγ by 12/15-LOX metabolites and, thus, the induction of PPARγ itself and target gene expression in multiple cells and tissues (28, 30, 31). These data prompted us to examine the possible link of them in brain tissue in the setting of ischemia. Our findings, for the first time, reported 12/15-LOX-derived metabolites 12(S)- and 15(S)-HETE can induce PPARγ expression and activity in ischemic brain and this action is beneficial to ischemic insult. Indeed, the endogenous activation of PPARγ after cerebral ischemia has been observed previously by us and others (26, 40, 45). Furthermore, the infarction size was demonstrated to be increased by the treatment of PPARγ antagonist in the absence of exogenous PPARγ agonist, suggesting that endogenous PPARγ activation is protective and can mitigate the effects of cerebral ischemia (40). Consistently, using neuronal PPARγ-deficient mice, Zhao et al. (26) showed that neuronal PPARγ deficiency is associated with augmented ischemic damage in response to MCAO. This data also indicates that an endogenous PPARγ pathway exists in the brain and is important in self-defense of the brain against ischemic injury. Thus, our data might help to explain, in part, the mechanism underlying the PPARγ activation in ischemic brain. However, it is noteworthy that this endogenous activation of PPARγ is likely in relatively low level and unable to confer sufficient neuroprotection in restricting the infarct development, if without enhancement by the PPARγ activator treated exogenously.

The protective PPARγ activation is also observed by other AA metabolites in the brain. For example, lipoxin A4, one of the AA products formed via 5-LOX, has been shown to have PPARγ agonistic actions and neuroprotection following experimental stroke, and to increase PPARγ transcriptional activity in isolated nuclei from rat brain cortex (46). The similar protective effects and PPARγ activation can be produced by 15d-PGJ2, one of the AA-derived products via the cyclooxygenase pathway, treated during brain ischemia in vivo and in vitro (36, 47, 48). Even AA, from which 12(S)- and 15(S)-HETE are derived, has been shown to be neuroprotective against oxidative stress on hippocampal slices through a process involving PPARγ signaling (33). Therefore, the PPARγ-dependent mechanism is not selective for 12/15-LOX and its 12(S)- and 15(S)-HETE products. Moreover, DHA and its derived products (resolvin D1 and neuroprotectin D1) have also been demonstrated to elicit the beneficial effects in vivo and vitro through a PPARγ-mediated mechanism (49–51). These data suggest that many endogenous fatty acid metabolites can activate PPARγ and PPARγ activation underlies their potential neuroprotective actions in the brain. This is also supported by the recent report showing a fatty acid binding pocket in the crystal structure of the PPARγ ligand binding domain. This pocket confers remarkable versatility in ligand binding, such that many different fatty acids and their derivatives can be accommodated (52).

Fig. 3. 12(S)-HETE and 15(S)-HETE inhibited the induction of COX-2, iNOS, and NF-κB in ischemic brain. Focal ischemia was induced by transient MCAO. 12(S)-HETE or 15(S)-HETE (10, 15, and 20 μg) or vehicle was injected icv 30 min before the onset of MCAO. The COX-2 and iNOS protein levels, NO content, and NF-κB activation in ipsilateral (ischemic) cortex were estimated at 24 h post-MCAO. Data are expressed as mean ± SEM; n = 8/group; $*P < 0.05$ versus sham-operated rats (Sham), $\#P < 0.05$ versus vehicle-treated ischemic rats (Veh). A: Western blot analysis of the protein levels of COX-2 and iNOS. The bar graph indicates the densitometric values of COX-2 or iNOS protein (normalized to GAPDH levels). B: The NO level estimated by the content of NO end product nitrate/nitrite. Results are expressed as nanomoles nitrate/nitrites per milligram protein. C: The effect of 12(S)-HETE or 15(S)-HETE (20 μg) on NF-κB activation measured by NF-κB DNA binding activity.

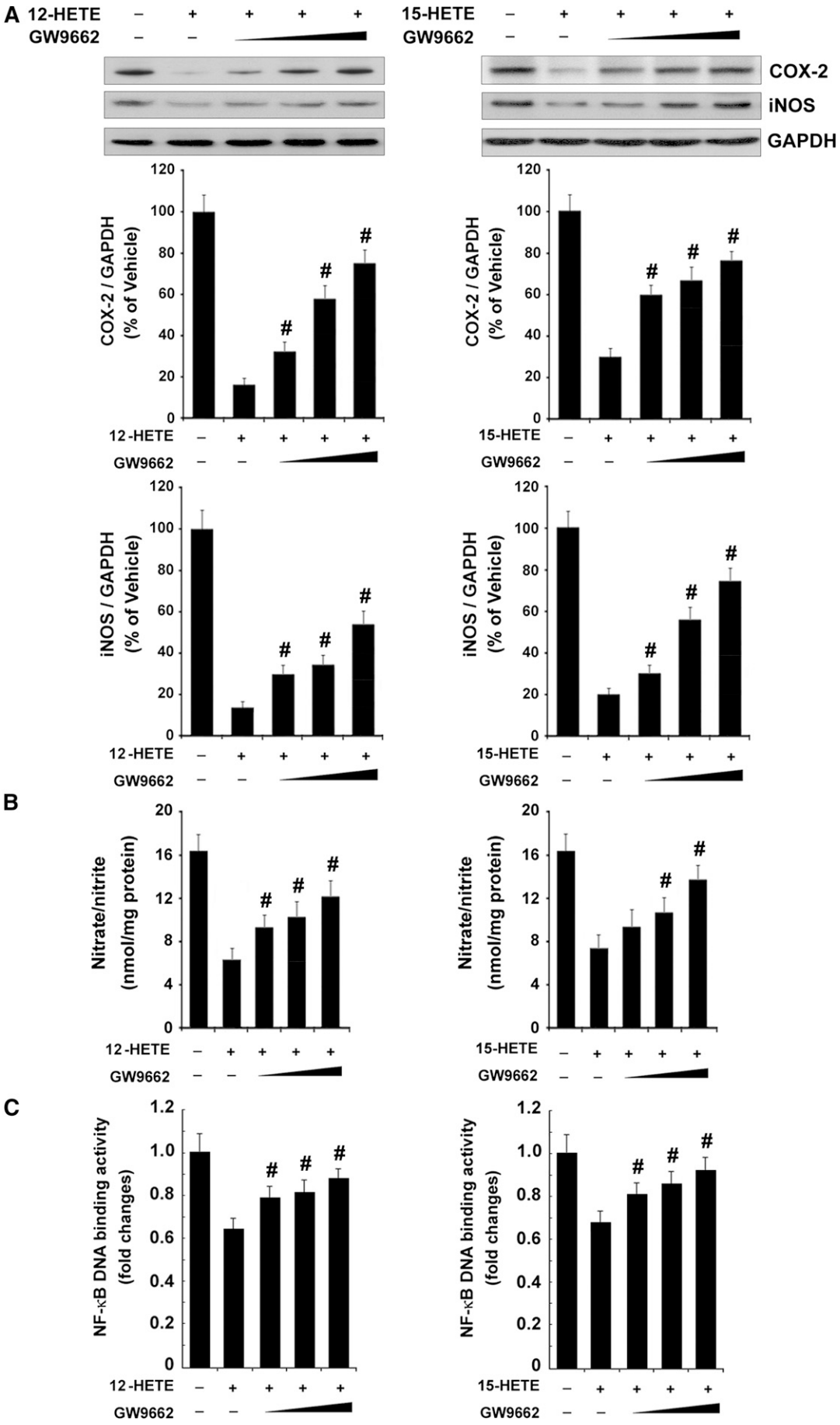
A
12-HETE
GW9662
15-HETE
COX-2
iNOS
GAPDH
COX-2 / GAPDH (% of Vehicle)
iNOS / GAPDH (% of Vehicle)
B
Nitrate/nitrite (nmol/mg protein)
C
NF-κB DNA binding activity (fold changes)

Extracellular free 12(S)- and 15(S)-HETE are known to be incorporated into membrane phospholipids (53, 54). The total 12(S)- and 15(S)-HETE detected in ischemic brain (Fig. 1D) in our study are supposed to involve both the free and esterified forms of them. However, it should be noted that ischemia induces the activation of phospholipase A2, the enzyme responsible for the massive hydrolysis of membrane phospholipids and release of unesterified fatty acids during cerebral ischemia (55, 56). Thus, we speculated that the majority of 12(S)- and 15(S)-HETE in ischemic brain (Fig. 1D) may be in free (unesterified) form, because the newly incorporated HETEs will be released by the action of phospholipase A2, if the incorporation of HETEs into membrane phospholipids occurs following ischemic injury.

In the ischemic brain, PPARγ immunoreactivity has been evidenced mainly in neurons (36, 40) and also in astrocytes, microglia (57), and other cells (58). In our data, most of the cells with 12/15-LOX staining also demonstrated positive immunoreactivity for the neuronal marker, which is consistent with the previous reports (14, 15, 59). Additionally, a G protein-coupled plasma membrane receptor has been identified for 12(S)- and 15(S)-HETE (41, 60). Based on these findings, we propose that, like other AA-derived eicosanoids (61–63), 12(S)-HETE and 15(S)-HETE function as autocrine and paracrine molecules, trigger PPARγ activation following their generation and secretion from neuronal 12/15-LOX, and thereby inhibit COX-2 and iNOS expression, as well as NF-κB activation in neurons, microglia, and other cells in the local environment. In addition, as autocrine and paracrine mediators, much higher localized concentrations of 12(S)-HETE and 15(S)-HETE are likely to occur in the microenvironment of cells that produce them. It is also possible that 12(S)-HETE and 15(S)-HETE can synergize with each other or with other 12/15-LOX derivatives (like 13-HODE) to regulate PPARγ in local ischemic region.

The mechanistic basis for the anti-inflammatory property of PPARγ has been investigated. Among several pathways, inhibition of the transcriptional activity of NF-κB is commonly involved (27, 64–67). NF-κB is an essential transcription factor necessary for iNOS and COX-2 gene transcription. The iNOS and COX-2 promoter comprises the binding sites for transcription factor NF-κB (68–70). Consistently, in the present study, the concomitant suppression in COX-2, iNOS, and NF-κB was observed in the ischemic brain by the action of either 12(S)-HETE or 15(S)-HETE. PPARγ has been reported to interfere with the NF-κB signaling pathway by preventing the binding of NF-κB protein to its target sequences (71). Furthermore, PPARγ can interact with NF-κB subunit p65 resulting in the reduction of p65 nuclear translocation (27). Accordingly, we assume that the suppression of pro-inflammatory proteins COX-2 and iNOS by the two metabolites is most likely dependent upon the inhibition of the NF-κB pathway.

In addition to PPARγ, several fatty acids also bind to PPARα (72, 73), and activation of this isoform of PPARs can afford neuroprotection from ischemic injury by anti-inflammatory mechanism (74, 75). In the present study, we cannot exclude the possibility that PPARα activation is involved in the actions of 12(S)- and 15(S)-HETE. Glutamate excitotoxicity is one of the critical components of cerebral ischemic pathology, and 12(S)- and 15(S)-HETE have been proven to be able to protect neurons from glutamate excitotoxicity by reducing calcium influx through voltage-gated channels (41). Future studies are needed to determine the exact signaling pathway central for the action of 12(S)- and 15(S)-HETE in ischemic injury of the brain.

The data presented here seem to conflict with the previous reports describing the detrimental effects of 12/15-LOX, and the protective effects of inhibiting 12/15-LOX in ischemic insult of the brain (14, 15, 76). Several reasons may explain this discrepancy: *1*) The biology of 12/15-LOX is complicated, because it has multiple catalytic activities, including hydroperoxidase activity, leukotriene synthase activity, lipoxin synthase activity, and hepoxilin synthase activity [for review see (77)]. In addition to producing 12(S)- and 15(S)-HETE, the enzyme is involved in the biosynthesis of lipoxins, hepoxilins, and other products. It is likely that 12/15-LOX-inhibiting or knockout mice are deficient in a complex mixture of lipid mediators that have been proven to mediate both pro- and anti-inflammatory pathways [for review see (78, 79)]. Thus, the interactive balance of these products probably dictates the eventual role of the 12/15-LOX pathway in the brain injury. This means 12/15-LOX and its individual metabolites may differ in their effects following cerebral ischemia. *2*) In addition to 12(S)- and 15(S)-HETE, the 12/15-LOX products of AA also include 12(S)- and 15(S)-hydroperoxyeicosatetraenoic acid (HPETE), the precursors of 12(S)- and 15(S)-HETE. Following synthesis, 12(S)- and 15(S)-HPETE are reduced by phospholipid glutathione peroxidase to form the corresponding HETEs. Several sources of evidence support the idea that the precursors, but not 12(S)- and 15(S)-HETE, are the metabolites implicated in the 12/15-LOX-dependent pathological process of cells (80–83). Moreover, phospholipid glutathione peroxidase in the 12/15-LOX pathway is a GSH-dependent peroxidase (84). Although the reduction of HPETEs to

Fig. 4. PPARγ antagonist, GW9662, reversed the suppressive effects of 12(S)-HETE and 15(S)-HETE on COX-2, iNOS, and NF-κB. Focal ischemia was induced by transient MCAO. Rats were injected ip with increasing concentrations (1, 2, and 4 mg/kg) of GW9662 30 min before the exposure to 12(S)- or 15(S)-HETE (20 μg) and MCAO. The COX-2 and iNOS protein levels, NO content, and NF-κB activation in ipsilateral (ischemic) cortex were estimated at 24 h post-MCAO. Data are expressed as mean ± SEM; n = 8/group; #$P < 0.05$ versus 12(S)-HETE- or 15(S)-HETE-treated rats alone. A: Western blot analysis of the protein levels of COX-2 and iNOS. The bar graph indicates the densitometric values of COX-2 or iNOS protein (normalized to GAPDH levels). B: The NO level estimated by the content of NO end product nitrate/nitrite. Results are expressed as nanomoles nitrates/nitrites per milligram protein. C: NF-κB activation measured by NF-κB DNA binding activity.

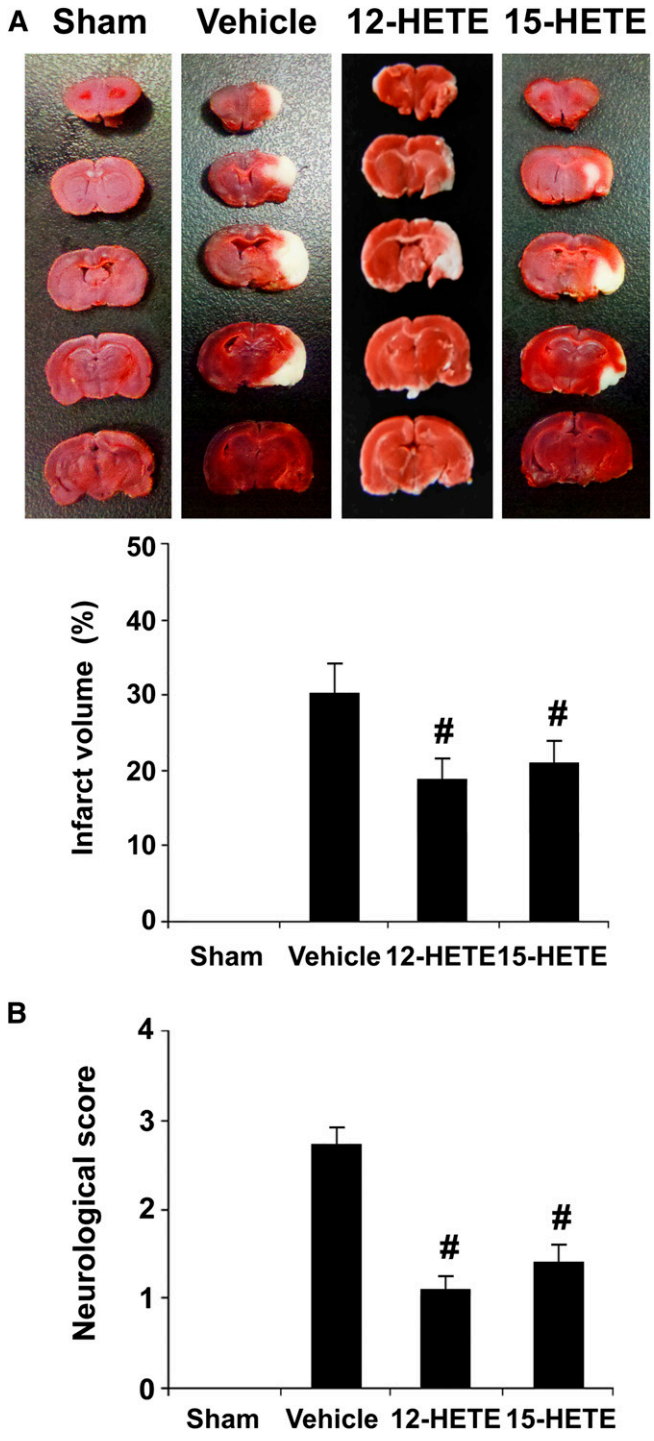

Fig. 5. 12(S)-HETE and 15(S)-HETE decreased infarct volume and improved neurological deficits. Focal ischemia was induced by transient MCAO. 12(S)-HETE (20 μg), 15(S)-HETE (20 μg), or vehicle was injected icv 30 min before the onset of 90 min MCAO. The infarct volume and neurological deficits were measured at 24 h after MCAO. Data are expressed as mean ± SEM; n = 8/group; #$P < 0.05$ versus vehicle-treated ischemic rats. A: The infarct volume measured by TTC staining. The bar graph illustrates the infarct volume quantified as percentage area of non-ischemic hemisphere. B: Neurological deficit scores. Neurological deficits were examined and scored on a grading scale of zero to four, which includes the assessment of motor deficits contralateral to the injured hemisphere and observation of circling behavior. Rats displaying better neurological outcome received lower neurological scores.

HETEs is very rapid, GSH decrease is able to inhibit the reduction of endogenous HPETE to HETE (80, 85). The increases in both HPETE half-life and its toxicity have been observed in neurons under GSH-depleted conditions (80, 81). This suggests that toxicity of HPETE may be greatly enhanced in several pathologies in which GSH decrease has been documented, such as stroke. *3*) In the oxidative injury of neural cells, the enzyme 12/15-LOX has been proven to be able to directly attack mitochondria, leading to cytochrome c release and production of reactive oxygen species. And furthermore, these events can all be replicated by incubation of 12/15-LOX with mitochondria in vitro, without the need to add other cytosolic factors (86). These data suggest 12/15-LOX itself could be the source of intracellular reactive oxygen species and the 12/15-LOX metabolites may not be absolutely required for its damaging effects during oxidative stress.

In summary, we have provided data suggesting that following ischemia, the induction of 12/15-LOX metabolites, 12(S)- and 15(S)-HETE, may associate with the activation of PPARγ and downregulate brain ischemia-induced pro-inflammatory signaling. They raise the intriguing possibility that the induction of the 12/15-LOX pathway may exert counterbalancing influences on brain ischemic insult, which may be of self-defense biological importance to the ischemic brain.

REFERENCES

1. Brash, A. R. 1999. Lipoxygenases: occurrence, functions, catalysis, and acquisition of substrate. *J. Biol. Chem.* **274:** 23679–23682.
2. Dobrian, A. D., D. C. Lieb, B. K. Cole, D. A. Taylor-Fishwick, S. K. Chakrabarti, and J. L. Nadler. 2011. Functional and pathological roles of the 12- and 15-lipoxygenases. *Prog. Lipid Res.* **50:** 115–131.
3. Nishiyama, M., H. Okamoto, T. Watanabe, T. Hori, T. Hada, N. Ueda, S. Yamamoto, H. Tsukamoto, K. Watanabe, and T. Kirino. 1992. Localization of arachidonate 12-lipoxygenase in canine brain tissues. *J. Neurochem.* **58:** 1395–1400.
4. Nishiyama, M., T. Watanabe, N. Ueda, H. Tsukamoto, and K. Watanabe. 1993. Arachidonate 12-lipoxygenase is localized in neurons, glial cells, and endothelial cells of the canine brain. *J. Histochem. Cytochem.* **41:** 111–117.
5. Shimizu, T., and L. S. Wolfe. 1990. Arachidonic acid cascade and signal transduction. *J. Neurochem.* **55:** 1–15.
6. Praticò, D., V. Zhukareva, Y. Yao, K. Uryu, C. D. Funk, J. A. Lawson, J. Q. Trojanowski, and V. M. Lee. 2004. 12/15-Lipoxygenase is increased in Alzheimer's disease: possible involvement in brain oxidative stress. *Am. J. Pathol.* **164:** 1655–1662.
7. Watanabe, T., J. F. Medina, J. Z. Haeggström, O. Rådmark, and B. Samuelsson. 1993. Molecular cloning of a 12-lipoxygenase cDNA from rat brain. *Eur. J. Biochem.* **212:** 605–612.
8. Piomelli, D., A. Volterra, N. Dale, S. A. Siegelbaum, E. R. Kandel, J. H. Schwartz, and F. Belardetti. 1987. Lipoxygenase metabolites of arachidonic acid as second messengers for presynaptic inhibition of Aplysia sensory cells. *Nature.* **328:** 38–43.
9. Ruehr, M. L., L. Zhang, and R. V. Dorman. 1997. Lipid-dependent modulation of Ca2+ availability in isolated mossy fiber nerve endings. *Neurochem. Res.* **22:** 1215–1222.
10. Chabot, C., J. Gagne, C. Giguere, J. Bernard, M. Baudry, and G. Massicotte. 1998. Bidirectional modulation of AMPA receptor properties by exogenous phospholipase A2 in the hippocampus. *Hippocampus.* **8:** 299–309.
11. Manzoni, O. J., and J. T. Williams. 1999. Presynaptic regulation of glutamate release in the ventral tegmental area during morphine withdrawal. *J. Neurosci.* **19:** 6629–6636.
12. Freeman, E. J., D. S. Damron, D. M. Terrian, and R. V. Dorman. 1991. 12-Lipoxygenase products attenuate the glutamate release

and Ca2+ accumulation evoked by depolarization of hippocampal mossy fiber nerve endings. *J. Neurochem.* **56:** 1079–1082.
13. Yigitkanli, K., A. Pekcec, H. Karatas, S. Pallast, E. Mandeville, N. Joshi, N. Smirnova, I. Gazaryan, R. R. Ratan, J. L. Witztum, et al. 2013. Inhibition of 12/15-lipoxygenase as therapeutic strategy to treat stroke. *Ann. Neurol.* **73:** 129–135.
14. van Leyen, K., H. Y. Kim, S. R. Lee, G. Jin, K. Arai, and E. H. Lo. 2006. Baicalein and 12/15-lipoxygenase in the ischemic brain. *Stroke.* **37:** 3014–3018.
15. Jin, G., K. Arai, Y. Murata, S. Wang, M. F. Stins, E. H. Lo, and K. van Leyen. 2008. Protecting against cerebrovascular injury: contributions of 12/15-lipoxygenase to edema formation after transient focal ischemia. *Stroke.* **39:** 2538–2543.
16. Bazan, N. G., V. L. Marcheselli, and K. Cole-Edwards. 2005. Brain response to injury and neurodegeneration: endogenous neuroprotective signaling. *Ann. N. Y. Acad. Sci.* **1053:** 137–147.
17. Belayev, L., L. Khoutorova, K. D. Atkins, and N. G. Bazan. 2009. Robust docosahexaenoic acid-mediated neuroprotection in a rat model of transient, focal cerebral ischemia. *Stroke.* **40:** 3121–3126.
18. Marcheselli, V. L., S. Hong, W. J. Lukiw, X. H. Tian, K. Gronert, A. Musto, M. Hardy, J. M. Gimenez, N. Chiang, C. N. Serhan, et al. 2003. Novel docosanoids inhibit brain ischemia-reperfusion-mediated leukocyte infiltration and pro-inflammatory gene expression. *J. Biol. Chem.* **278:** 43807–43817.
19. Lakshmi, S. P., A. T. Reddy, Y. Zhang, F. C. Sciurba, R. K. Mallampalli, S. R. Duncan, and R. C. Reddy. 2014. Down-regulated peroxisome proliferator-activated receptor gamma (PPARgamma) in lung epithelial cells promotes a PPARgamma agonist-reversible proinflammatory phenotype in Chronic Obstructive Pulmonary Disease (COPD). *J. Biol. Chem.* **289:** 6383–6393.
20. Ballesteros, I., M. I. Cuartero, J. M. Pradillo, J. de la Parra, A. Pérez-Ruiz, A. Corbí, M. Ricote, J. A. Hamilton, M. Sobrado, J. Vivancos, et al. 2014. Rosiglitazone-induced CD36 up-regulation resolves inflammation by PPARgamma and 5-LO-dependent pathways. *J. Leukoc. Biol.* **95:** 587–598.
21. Ramkalawan, H., Y. Z. Wang, A. Hurbungs, Y. F. Yang, F. F. Tian, W. B. Zhou, J. Li, H. Yang, B. Xiao, and W. Zhang. 2012. Pioglitazone, PPARgamma agonist, attenuates experimental autoimmune neuritis. *Inflammation.* **35:** 1338–1347.
22. Sundararajan, S., J. L. Gamboa, N. A. Victor, E. W. Wanderi, W. D. Lust, and G. E. Landreth. 2005. Peroxisome proliferator-activated receptor-gamma ligands reduce inflammation and infarction size in transient focal ischemia. *Neuroscience.* **130:** 685–696.
23. Zhao, Y., A. Patzer, P. Gohlke, T. Herdegen, and J. Culman. 2005. The intracerebral application of the PPARgamma-ligand pioglitazone confers neuroprotection against focal ischaemia in the rat brain. *Eur. J. Neurosci.* **22:** 278–282.
24. Collino, M., M. Aragno, R. Mastrocola, M. Gallicchio, A. C. Rosa, C. Dianzani, O. Danni, C. Thiemermann, and R. Fantozzi. 2006. Modulation of the oxidative stress and inflammatory response by PPAR-gamma agonists in the hippocampus of rats exposed to cerebral ischemia/reperfusion. *Eur. J. Pharmacol.* **530:** 70–80.
25. Luo, Y., W. Yin, A. P. Signore, F. Zhang, Z. Hong, S. Wang, S. H. Graham, and J. Chen. 2006. Neuroprotection against focal ischemic brain injury by the peroxisome proliferator-activated receptor-gamma agonist rosiglitazone. *J. Neurochem.* **97:** 435–448.
26. Zhao, X., R. Strong, J. Zhang, G. Sun, J. Z. Tsien, Z. Cui, J. C. Grotta, and J. Aronowski. 2009. Neuronal PPARgamma deficiency increases susceptibility to brain damage after cerebral ischemia. *J. Neurosci.* **29:** 6186–6195.
27. Zhang, H. L., M. Xu, C. Wei, A. P. Qin, C. F. Liu, L. Z. Hong, X. Y. Zhao, J. Liu, and Z. H. Qin. 2011. Neuroprotective effects of pioglitazone in a rat model of permanent focal cerebral ischemia are associated with peroxisome proliferator-activated receptor gamma-mediated suppression of nuclear factor-kappaB signaling pathway. *Neuroscience.* **176:** 381–395.
28. Li, Q., Y. P. Cheon, A. Kannan, S. Shanker, I. C. Bagchi, and M. K. Bagchi. 2004. A novel pathway involving progesterone receptor, 12/15-lipoxygenase-derived eicosanoids, and peroxisome proliferator-activated receptor gamma regulates implantation in mice. *J. Biol. Chem.* **279:** 11570–11581.
29. Altmann, R., M. Hausmann, T. Spöttl, M. Gruber, A.W. Bull, K. Menzel, D. Vogl, H. Herfarth, J. Schölmerich, W. Falk, and G. Rogler. 2007. 13-Oxo-ODE is an endogenous ligand for PPARgamma in human colonic epithelial cells. *Biochem. Pharmacol.* 74:612–622.
30. Berry, A., P. Balard, A. Coste, D. Olagnier, C. Lagane, H. Authier, F. Benoit-Vical, J. C. Lepert, J. P. Séguéla, J. F. Magnaval, et al. 2007. IL-13 induces expression of CD36 in human monocytes through PPARgamma activation. *Eur. J. Immunol.* **37:** 1642–1652.
31. Limor, R., O. Sharon, E. Knoll, A. Many, G. Weisinger, and N. Stern. 2008. Lipoxygenase-derived metabolites are regulators of peroxisome proliferator-activated receptor gamma-2 expression in human vascular smooth muscle cells. *Am. J. Hypertens.* **21:** 219–223.
32. Chabane, N., N. Zayed, M. Benderdour, J. Martel-Pelletier, J. P. Pelletier, N. Duval, and H. Fahmi. 2009. Human articular chondrocytes express 15-lipoxygenase-1 and -2: potential role in osteoarthritis. *Arthritis Res. Ther.* **11:** R44.
33. Wang, Z. J., C. L. Liang, G. M. Li, C. Y. Yu, and M. Yin. 2006. Neuroprotective effects of arachidonic acid against oxidative stress on rat hippocampal slices. *Chem. Biol. Interact.* **163:** 207–217.
34. Sun, L., L. Yang, Y. Fu, J. Han, Y. Xu, H. Liang, and Y. Cheng. 2013. Capacity of HSYA to inhibit nitrotyrosine formation induced by focal ischemic brain injury. *Nitric Oxide.* **35:** 144–151.
35. Churi, S. B., O. S. Abdel-Aleem, K. K. Tumber, H. Scuderi-Porter, and B. K. Taylor. 2008. Intrathecal rosiglitazone acts at peroxisome proliferator-activated receptor-gamma to rapidly inhibit neuropathic pain in rats. *J. Pain.* **9:** 639–649.
36. Ou, Z., X. Zhao, L. A. Labiche, R. Strong, J. C. Grotta, O. Herrmann, and J. Aronowski. 2006. Neuronal expression of peroxisome proliferator-activated receptor-gamma (PPARgamma) and 15d-prostaglandin J2–mediated protection of brain after experimental cerebral ischemia in rat. *Brain Res.* **1096:** 196–203.
37. Lesuisse, C., and L. J. Martin. 2002. Long-term culture of mouse cortical neurons as a model for neuronal development, aging, and death. *J. Neurobiol.* **51:** 9–23.
38. Tugwood, J. D., I. Issemann, R. G. Anderson, K. R. Bundell, W. L. McPheat, and S. Green. 1992. The mouse peroxisome proliferator activated receptor recognizes a response element in the 5′ flanking sequence of the rat acyl CoA oxidase gene. *EMBO J.* **11:** 433–439.
39. Dalby, B., S. Cates, A. Harris, E. C. Ohki, M. L. Tilkins, P. J. Price, and V. C. Ciccarone. 2004. Advanced transfection with Lipofectamine 2000 reagent: primary neurons, siRNA, and high-throughput applications. *Methods.* **33:** 95–103.
40. Victor, N. A., E. W. Wanderi, J. Gamboa, X. Zhao, J. Aronowski, K. Deininger, W. D. Lust, G. E. Landreth, and S. Sundararajan. 2006. Altered PPARgamma expression and activation after transient focal ischemia in rats. *Eur. J. Neurosci.* **24:** 1653–1663.
41. Hampson, A. J., and M. Grimaldi. 2002. 12-hydroxyeicosatetrenoate (12-HETE) attenuates AMPA receptor-mediated neurotoxicity: evidence for a G-protein-coupled HETE receptor. *J. Neurosci.* **22:** 257–264.
42. Romera, C., O. Hurtado, J. Mallolas, M. P. Pereira, J. R. Morales, A. Romera, J. Serena, J. Vivancos, F. Nombela, P. Lorenzo, et al. 2007. Ischemic preconditioning reveals that GLT1/EAAT2 glutamate transporter is a novel PPARgamma target gene involved in neuroprotection. *J. Cereb. Blood Flow Metab.* **27:** 1327–1338.
43. Candelario-Jalil, E., A. González-Falcón, M. García-Cabrera, D. Alvarez, S. Al-Dalain, G. Martínez, O. S. León, and J. E. Springer. 2003. Assessment of the relative contribution of COX-1 and COX-2 isoforms to ischemia-induced oxidative damage and neurodegeneration following transient global cerebral ischemia. *J. Neurochem.* **86:** 545–555.
44. Lerouet, D., V. Beray-Berthat, B. Palmier, M. Plotkine, and I. Margaill. 2002. Changes in oxidative stress, iNOS activity and neutrophil infiltration in severe transient focal cerebral ischemia in rats. *Brain Res.* **958:** 166–175.
45. Xu, Y. W., L. Sun, H. Liang, G. M. Sun, and Y. Cheng. 2010. 12/15-Lipoxygenase inhibitor baicalein suppresses PPAR gamma expression and nuclear translocation induced by cerebral ischemia/reperfusion. *Brain Res.* **1307:** 149–157.
46. Sobrado, M., M. P. Pereira, I. Ballesteros, O. Hurtado, D. Fernandez-Lopez, J. M. Pradillo, J. R. Caso, J. Vivancos, F. Nombela, J. Serena, et al. 2009. Synthesis of lipoxin A4 by 5-lipoxygenase mediates PPARgamma-dependent, neuroprotective effects of rosiglitazone in experimental stroke. *J. Neurosci.* **29:** 3875–3884.
47. Lin, T. N., W. M. Cheung, J. S. Wu, J. J. Chen, H. Lin, J. J. Chen, J. Y. Liou, S. K. Shyue, and K. K. Wu. 2006. 15d-prostaglandin J2 protects brain from ischemia-reperfusion injury. *Arterioscler. Thromb. Vasc. Biol.* **26:** 481–487.
48. Du, H., X. Chen, J. Zhang, and C. Chen. 2011. Inhibition of COX-2 expression by endocannabinoid 2-arachidonoylglycerol is mediated via PPAR-gamma. *Br. J. Pharmacol.* **163:** 1533–1549.
49. Zhao, Y., F. Calon, C. Julien, J. W. Winkler, N. A. Petasis, W. J. Lukiw, and N. G. Bazan. 2011. Docosahexaenoic acid-derived neuroprotectin D1 induces neuronal survival via secretase- and

PPARgamma-mediated mechanisms in Alzheimer's disease models. *PLoS ONE.* **6:** e15816.
50. Liao, Z., J. Dong, W. Wu, T. Yang, T. Wang, L. Guo, L. Chen, D. Xu, and F. Wen. 2012. Resolvin D1 attenuates inflammation in lipopolysaccharide-induced acute lung injury through a process involving the PPARγ/NF-κB pathway. *Respir. Res.* **13:** 110.
51. Li, H., X. Z. Ruan, S. H. Powis, R. Fernando, W. Y. Mon, D. C. Wheeler, J. F. Moorhead, and Z. Varghese. 2005. EPA and DHA reduce LPS-induced inflammation responses in HK-2 cells: evidence for a PPAR-gamma-dependent mechanism. *Kidney Int.* **67:** 867–874.
52. Itoh, T., L. Fairall, K. Amin, Y. Inaba, A. Szanto, B. L. Balint, L. Nagy, K. Yamamoto, and J. W. Schwabe. 2008. Structural basis for the activation of PPARgamma by oxidized fatty acids. *Nat. Struct. Mol. Biol.* **15:** 924–931.
53. Brezinski, M. E., and C. N. Serhan. 1990. Selective incorporation of (15S)-hydroxyeicosatetraenoic acid in phosphatidylinositol of human neutrophils: agonist-induced deacylation and transformation of stored hydroxyeicosanoids. *Proc. Natl. Acad. Sci. USA.* **87:** 6248–6252.
54. Spector, A. A., J. A. Gordon, and S. A. Moore. 1988. Hydroxyeicosatetraenoic acids (HETEs). *Prog. Lipid Res.* **27:** 271–323.
55. Umemura, A., H. Mabe, H. Nagai, and F. Sugino. 1992. Action of phospholipases A2 and C on free fatty acid release during complete ischemia in rat neocortex. Effect of phospholipase C inhibitor and N-methyl-D-aspartate antagonist. *J. Neurosurg.* **76:** 648–651.
56. Adibhatla, R. M., J. F. Hatcher, and R. J. Dempsey. 2003. Phospholipase A2, hydroxyl radicals, and lipid peroxidation in transient cerebral ischemia. *Antioxid. Redox Signal.* **5:** 647–654.
57. Carniglia, L., D. Durand, C. Caruso, and M. Lasaga. 2013. Effect of NDP-alpha-MSH on PPAR-gamma and -beta expression and anti-inflammatory cytokine release in rat astrocytes and microglia. *PLoS ONE.* **8:** e57313.
58. Yin, K. J., Y. Fan, M. Hamblin, J. Zhang, T. Zhu, S. Li, J. R. Hawse, M. Subramaniam, C. Z. Song, R. Urrutia, et al. 2013. KLF11 mediates PPARgamma cerebrovascular protection in ischaemic stroke. *Brain.* **136:** 1274–1287.
59. Pallast, S., K. Arai, A. Pekcec, K. Yigitkanli, Z. Yu, X. Wang, E. H. Lo, and K. van Leyen. 2010. Increased nuclear apoptosis-inducing factor after transient focal ischemia: a 12/15-lipoxygenase-dependent organelle damage pathway. *J. Cereb. Blood Flow Metab.* **30:** 1157–1167.
60. Guo, Y., W. Zhang, C. Giroux, Y. Cai, P. Ekambaram, A. K. Dilly, A. Hsu, S. Zhou, K. R. Maddipati, J. Liu, et al. 2011. Identification of the orphan G protein-coupled receptor GPR31 as a receptor for 12-(S)-hydroxyeicosatetraenoic acid. *J. Biol. Chem.* **286:** 33832–33840.
61. Yin, H., Y. Zhou, M. Zhu, S. Hou, Z. Li, H. Zhong, J. Lu, T. Meng, J. Wang, L. Xia, et al. 2013. Role of mitochondria in programmed cell death mediated by arachidonic acid-derived eicosanoids. *Mitochondrion.* **13:** 209–224.
62. Luo, M., N. Flamand, and T. G. Brock. 2006. Metabolism of arachidonic acid to eicosanoids within the nucleus. *Biochim. Biophys. Acta.* **1761:** 618–625.
63. Spector, A. A. 2009. Arachidonic acid cytochrome P450 epoxygenase pathway. *J. Lipid Res.* **50(Suppl):** S52–S56.
64. Pascual, G., A. L. Fong, S. Ogawa, A. Gamliel, A. C. Li, V. Perissi, D. W. Rose, T. M. Willson, M. G. Rosenfeld, and C. K. Glass. 2005. A SUMOylation-dependent pathway mediates transrepression of inflammatory response genes by PPAR-gamma. *Nature.* **437:** 759–763.
65. Lee, K. S., S. R. Kim, S. J. Park, H. S. Park, K. H. Min, S. M. Jin, M. K. Lee, U. H. Kim, and Y. C. Lee. 2006. Peroxisome proliferator activated receptor-gamma modulates reactive oxygen species generation and activation of nuclear factor-kappaB and hypoxia-inducible factor 1alpha in allergic airway disease of mice. *J. Allergy Clin. Immunol.* **118:** 120–127.
66. Sung, B., S. Park, B. P. Yu, and H. Y. Chung. 2006. Amelioration of age-related inflammation and oxidative stress by PPARgamma activator: suppression of NF-kappaB by 2,4-thiazolidinedione. *Exp. Gerontol.* **41:** 590–599.
67. Kim, E. K., K. B. Kwon, B. S. Koo, M. J. Han, M. Y. Song, E. K. Song, M. K. Han, J. W. Park, D. G. Ryu, and B. H. Park. 2007. Activation of peroxisome proliferator-activated receptor-gamma protects pancreatic beta-cells from cytokine-induced cytotoxicity via NF kappaB pathway. *Int. J. Biochem. Cell Biol.* **39:** 1260–1275.
68. Lin, A. W., C. C. Chang, and C. C. McCormick. 1996. Molecular cloning and expression of an avian macrophage nitric-oxide synthase cDNA and the analysis of the genomic 5′-flanking region. *J. Biol. Chem.* **271:** 11911–11919.
69. Singer, C. A., K. J. Baker, A. McCaffrey, D. P. AuCoin, M. A. Dechert, and W. T. Gerthoffer. 2003. p38 MAPK and NF-kappaB mediate COX-2 expression in human airway myocytes. *Am. J. Physiol. Lung Cell. Mol. Physiol.* **285:** L1087–L1098.
70. Suh, Y., F. Afaq, J. J. Johnson, and H. Mukhtar. 2009. A plant flavonoid fisetin induces apoptosis in colon cancer cells by inhibition of COX2 and Wnt/EGFR/NF-kappaB-signaling pathways. *Carcinogenesis.* **30:** 300–307.
71. Chinetti, G., J. C. Fruchart, and B. Staels. 2000. Peroxisome proliferator-activated receptors (PPARs): nuclear receptors at the crossroads between lipid metabolism and inflammation. *Inflamm. Res.* **49:** 497–505.
72. Rodríguez-Cruz, M., A. R. Tovar, M. del Prado, and N. Torres. 2005. Molecular mechanisms of action and health benefits of polyunsaturated fatty acids. *Rev. Invest. Clin.* **57:** 457–472.
73. Kim, Y. I., S. Hirai, T. Goto, C. Ohyane, H. Takahashi, T. Tsugane, C. Konishi, T. Fujii, S. Inai, Y. Iijima, et al. 2012. Potent PPARalpha activator derived from tomato juice, 13-oxo-9,11-octadecadienoic acid, decreases plasma and hepatic triglyceride in obese diabetic mice. *PLoS ONE.* **7:** e31317.
74. Ouk, T., S. Gautier, M. Pétrault, D. Montaigne, X. Maréchal, I. Masse, J. C. Devedjian, D. Deplanque, M. Bastide, R. Nevière, et al. 2014. Effects of the PPAR-alpha agonist fenofibrate on acute and short-term consequences of brain ischemia. *J. Cereb. Blood Flow Metab.* **34:** 542–551.
75. Deplanque, D., P. Gelé, O. Pétrault, I. Six, C. Furman, M. Bouly, S. Nion, B. Dupuis, D. Leys, J. C. Fruchart, et al. 2003. Peroxisome proliferator-activated receptor-alpha activation as a mechanism of preventive neuroprotection induced by chronic fenofibrate treatment. *J. Neurosci.* **23:** 6264–6271.
76. Li, Y., P. Maher, and D. Schubert. 1997. A role for 12-lipoxygenase in nerve cell death caused by glutathione depletion. *Neuron.* **19:** 453–463.
77. Takata, S., M. Matsubara, P. G. Allen, P. A. Janmey, C. N. Serhan, and H. R. Brady. 1994. Remodeling of neutrophil phospholipids with 15(S)-hydroxyeicosatetraenoic acid inhibits leukotriene B4-induced neutrophil migration across endothelium. *J. Clin. Invest.* **93:** 499–508.
78. Kühn, H., and V. B. O'Donnell. 2006. Inflammation and immune regulation by 12/15-lipoxygenases. *Prog. Lipid Res.* **45:** 334–356.
79. Wittwer, J., and M. Hersberger. 2007. The two faces of the 15-lipoxygenase in atherosclerosis. *Prostaglandins Leukot. Essent. Fatty Acids.* **77:** 67–77.
80. Canals, S., M. J. Casarejos, S. de Bernardo, E. Rodríguez-Martín, and M. A. Mena. 2003. Nitric oxide triggers the toxicity due to glutathione depletion in midbrain cultures through 12-lipoxygenase. *J. Biol. Chem.* **278:** 21542–21549.
81. Kramer, B. C., J. A. Yabut, J. Cheong, R. Jnobaptiste, T. Robakis, C. W. Olanow, and C. Mytilineou. 2004. Toxicity of glutathione depletion in mesencephalic cultures: a role for arachidonic acid and its lipoxygenase metabolites. *Eur. J. Neurosci.* **19:** 280–286.
82. Riccio, M. M., T. Matsumoto, J. J. Adcock, G. J. Douglas, D. Spina, and C. P. Page. 1997. The effect of 15-HPETE on airway responsiveness and pulmonary cell recruitment in rabbits. *Br. J. Pharmacol.* **122:** 249–256.
83. Lai, C. K., G. D. Phillips, J. R. Jenkins, and S. T. Holgate. 1990. The effect of inhaled 15-(s)-hydroxyeicosatetraenoic acid (15-HETE) on airway calibre and non-specific responsiveness in normal and asthmatic human subjects. *Eur. Respir. J.* **3:** 38–45.
84. Chang, W. C., J. Nakao, H. Orimo, and S. Murota. 1982. Effects of reduced glutathione on the 12-lipoxygenase pathways in rat platelets. *Biochem. J.* **202:** 771–776.
85. Ochi, H., I. Morita, and S. Murota. 1992. Roles of glutathione and glutathione peroxidase in the protection against endothelial cell injury induced by 15-hydroperoxyeicosatetraenoic acid. *Arch. Biochem. Biophys.* **294:** 407–411.
86. Pallast, S., K. Arai, X. Wang, E. H. Lo, and K. van Leyen. 2009. 12/15-Lipoxygenase targets neuronal mitochondria under oxidative stress. *J. Neurochem.* **111:** 882–889.